# IN-REACTOR PRECIPITATION AND FERRITIC TRANSFORMATION IN NEUTRON - IRRADIATED STAINLESS STEELS

by

D. L. Porter and E. L. Wood

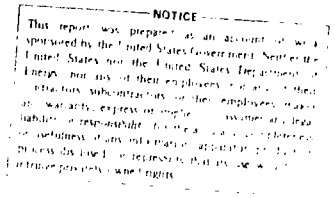


Prepared for

Workshop on

Solute Segregation and Phase Stability during Irradiation

Gatlinburg, Tennessee

November 1-3, 1978

U of C-AUA-USDOE

ARGONNE NATIONAL LABORATORY, ARGONNE, ILLINOIS

Operated under Contract W-31-109-Eng-38 for the

U. S. DEPARTMENT OF ENERGY

# IN-REACTOR PRECIPITATION AND FERRITIC TRANSFORMATION IN NEUTRON-IRRADIATED STAINLESS STEELS

## ABSTRACT

Ferritic transformation ($\gamma \rightarrow \alpha$) was observed in Type 304L, 20% cold-worked AISI 316, and solution-annealed AISI 316 stainless steels when subjected to fast neutron irradiation. Each material demonstrated an increasing propensity for transformation with increasing irradiation temperature between 400 and 550°C. Irradiation-induced segregation of Ni solute to precipitates was found not to influence the transformation kinetics in 304L. Similar composition data from 316 materials demonstrates a much greater temperature dependence of precipitation reactions in the process of matrix Ni depletion during neutron irradiation. The 316 data establishes a strong link between such depletion and the observed $\gamma \rightarrow \alpha$ transformation. Moreover, the lack of correlation between precipitate-related Ni depletion and the $\gamma \rightarrow \alpha$ transformation in 304L can be related to the fact that irradiation-induced voids nucleate very quickly in 304L steel during irradiation. These voids present preferential sites for Ni segregation through a defect trapping mechanism, and hence Ni segregates to voids rather than to precipitates, as evidenced by observed stable $\gamma$ shells around voids in areas of complete transformation.

# INTRODUCTION

## 1. Irradiation-induced $\gamma \rightarrow \alpha$ Transformation

Irradiation-induced $\gamma \rightarrow \alpha$ transformation has been observed previously in several metasable austenitic stainless steels, including 316,[1,2] 321[3] and 304L.[4] Comparison of these studies with a long-term out-of-reactor heat treatment of 321 steel[5], in which no transformation occurred, indicates that the observed transformations in radiation environments were indeed peculiar to a radiation environment and not merely accelerated by radiation damage. The study of 304L materials[4] illustrated that the transformation in this alloy was characterized by a nucleation and growth process, nucleating on faulted Frank loops and growing to consume all but shell-like regions of $\gamma$ around irradiation-produced voids within a given grain of the material. The transformation kinetics were found to be most accelerated near irradiation temperatures of 500°C, decreasing continuously with temperature to a nil rate near 400°C, despite the fact that $\gamma$-stability also decreases with temperature.

A similar temperature dependence was observed in a study of proton-irradiated 321 steel[3] where much less transformation occurred upon irradiation at 400°C than at 500°C.

## 2. Chemical Segregation

The observed temperature dependence of the forementioned phase transformation is interestingly similar to that observed for void swelling of these materials. That is, the most rapid void swelling

rates are observed at temperatures near those where the $\gamma \rightarrow \alpha$ transformation is most prevalent. Moreover, swelling investigations in austenitic stainless steels indicates that chemical segregation during irradiation plays a major role in determining void-swelling rates and the neutron fluence which can be accumulated before the onset of rapid void growth. Brager and Garner[6] have found that the time-dependent behavior of the void-swelling rate in Type 316 stainless steel is dominated by the time-dependent composition of the austenitic matrix. McVay et al.[7] have shown that swelling and creep in 316 materials are strongly correlated to the rate of carbosilicide precipitation. It is therefore not surprising that another composition-dependent factor, austenite stability, is found to show similar response to the temperature of the irradiation environment.

Chemical segregation during irradiation is likely to occur by both defect trapping and normal precipitation reactions. Defect trapping occurs as a result of the formation of energetically favorable defect complexes between over-or undersized solute atoms and radiation-induced defects (vacancies and interstitials). As a result of defect-solute coupling the possibility exists for solute redistribution by migration of the solutes against the defect flux. Okamoto and Wiedersich[8] have used these ideas to explain observed concentration build-ups of undersized solutes, Ni and Si, near defect sinks in stainless steel alloys. Likewise,

Potter et al.[9] have utilized similar explanations to describe observed formation of γ' particles ($Ni_3Si$) upon irradiation of Ni-Si alloys at temperatures and compositions where solid solutions are normally stable.[9,10] They further found that when Ni-Al alloys were irradiated, the stable $Ni_3Al$-γ' (which had been precipitated prior to irradiation) dissolved, proving that radiation-enhanced diffusion kinetics were not the cause of the observed effects.

Brager and Garner[11] demonstrated that neutron irradiation produces these same $Ni_3Si$ precipitates in Type 316 stainless steel at irradiation temperatures less than 525°C. They also found that above 525°C, precipitation of a carbosilicide - $M_{23}(C, Si)_6$ - predominates with an apparent spatial association between these precipitates and irradiation-induced voids. While $M_{23}C_6$ precipitation occurs normally in unirradiated 316 steel, the overall compositions are quite different. At 900°C the $M_{23}C_6$ precipitate has a composition near to $(Cr_{16}\ Fe_5\ Mo_2)\ C_6$[12,13] and these compositions vary slightly with precipitation temperature and initial matrix composition.[14] However, Brager and Garner[11] previously found that irradiation-induced carbosilicides had a composition of $(Fe_{10}Ni_7Cr_4Mo_2)$ $(C_3Si_3)$ at 525°C and $\phi t$ (E>0.1 Mev) = $4 \times 10^{26} n/m^2$. More recently these same investigators found that at 600°C and $\phi t = 9 \times 10^{26}$ $n/cm^2$, these precipitates had compositions near $(Cr_{10}Ni_6Fe_4Mo_3)$ $(C_3Si_3)$.[16] Under irradiation conditions, precipitate composition seems to vary much more widely and shows the presence of large amounts of unexpected elements, e.g. Ni and Si.

It is clear that chemical segregation in irradiated austenitic stainless steel may be observed in the formation of many precipitates,

some expected from normal phase equilibria, and some not. The chemical compositions of the precipitates provide indications of which solutes are being redistributed, perhaps by a defect-solute drag mechanism.

As the solutes are redistributed, material properties such as void swelling[15,16] and austenite phase stability[4] are affected. It is the purpose of this investigation to examine solute removal from the matrix of Types 316 and 304L stainless steels through precipitate chemical analysis. Observed $\gamma \rightarrow \alpha$ transformation in these alloys will be examined in light of these findings.

## 3. Materials and Procedures

The study was comprised of examination of three different irradiated* materials: solution-annealed AISI 316 stainless steel fueled cladding (Mark-II fuel elements), AISI 316 creep capsule material which had received either a solution-annealing or 20% cold-work treatment prior to irradiation, and Type 304L stainless steel unstressed-capsule material.[4] The nominal compositions of these materials appear in Table 1. Irradiation temperatures included a range from ~400-515°C for 304L, ~430-670°C for the 316 fueled cladding, and either 400°C or 550°C for the 316 creep capsule material.

---

*All materials were irradiated in the EBR-II reactor and all references to neutron fluence accumulations will refer to fast (E>0.1 MeV) fluences.

Transmission electron microscopy foils were cut from these specimens to examine precipitate formation and phase transformation. In addition, sections of capsule or cladding ($\sim$ 1 inch long) were used to examine carbosiilicide compsitions. This procedure consisted of electrolytically dissolving the maxtrix material in order to extract the precipitate phase ($\gamma'$- precipitates also dissolved during this process). Once extracted, the precipitates were electrolytically dissolved and their compositions determined using atomic absorption analysis. Data from this procedure consisted of weights of elemental ions (Fe, Cr, Mo, and Ni) which comprised the carbosilicide phase; the weights were then subsequently reduced to mole fractions so that representative compositions could be determined.

In addition, a crude magnetic check, using a hand magnet, was performed on each prethinned microscopy disc to check for possible phase transformation ($\gamma \rightarrow \alpha$). The prethinning operation removed $\sim$0.1-0.3 mm from each surface of the disc to eliminate any ferritic layer which may have resulted from in-reactor exposure to molten sodium. An electromagnetic device triggered to a precision balance apparatus allowed estimates of the degree of transformation. Weights of magnetic phase were determined by what voltage applied to the electromagnet was necessary to tip the balance. The voltages were compared to a calibration curve which had been determined using specimens containing known weights of magnetic phase.

## Results and Discussion

### 1. Ferritic Transformation

Figure 1 illustrates a typical transformation boundary between the parent $\gamma$ phase and the $\alpha$ product in Type 304L steel. Heavy faulting in the $\gamma$ phase just ahead of the interface is exemplary of the growth of the ferritic phase into the austenite matrix. Also illustrated are the austentic shells remaining around the irradiation-induced voids. A summary of the observed transformation characteristics appears in the Introduction of this paper. While these results have previously been reported,[4] evidence was lacking for the causes of the unexpected transformation, its unusual temperature dependence ($\gamma$ should be more stable at higher temperatures yet was found to transform to $\alpha$ more readily at higher irradiation temperatures), and the fact that austenite remained as shells around voids. Evidence for these effects will be discussed in this study.

The 316 materials studied here showed some similar transformation characteristics. The transformation was found to occur in both solution annealed (fueled and unfueled) and 20% cold-worked materials upon modest neutron exposures ($\sim 4 \times 10^{26} n/m^2$). However, this transformation occurred only upon irradiation at 550°C and no transformation could be detected in materials irradiated at 400°C to fluences approaching $6 \times 10^{26} n/m^2$. Furthermore, the solution annealed material was found to exhibit stronger magnetic response than cold-worked material after receiving similar fluences. As found in the study of 304L steel, the magnetic response increased with accumulated fluence, although estimates

of the degree of transformation indicated that even the most heavily transformed material was only 4-8% transformed. Similar estimates indicated that 304L material irradiated at 502°C and $\phi t = 7.6 \times 10^{26} n/m^2$, had transformed about 15% by volume.

Microstructural examinations of 304L material indicated that the transformation was nucleated on irradiation-induced faulted dislocation loops. These faulted regions provide the critical initial nucleation sites. Microstructural examinations, however, could not explain the observed temperature dependence or the reason for the retention of austentic phase near voids. An accessory phenomenon, such as irradiation-induced chemical segregation (specifically of Ni) was thought to exist and therefore extensive chemical analyses of precipitate phases were performed.

Retention of $\gamma$ phase near irradiation-induced voids can be best explained by comparison to other work. Okamoto and Wiedersich[8] have shown that similar microstructures, namely the existence of a second phase around voids, were formed in Ni-ion irradiated stainless steels. They have attributed this to a defect trapping mechanism in which undersized solute atoms (Ni and Si) are transported to point defect sinks, such as voids, through formation of point defect-solute complexes. A similar phenomenon would explain the occurrence of austenitic shells around voids if Ni, a potent $\gamma$ stabilizer, is deposited near voids. Assuming such segregation occurs, the enhanced Ni mobility may also be reflected in precipitate compositions. The temperature dependence of such compositions may then demonstrate a contribution of Ni segregation

to the temperature dependence of the ferritic transformation. This could be especially important in 316 materials where the higher matrix content of Ni makes the occurrence of $\gamma \rightarrow \alpha$ transformation much less expected than in 304L. The question can then be answered as to whether the temperature dependence is inherent to the transformation or if the segregation of Ni contributes to such a correlation.

Carbosilicide Analyses

X-ray analysis has indicated that extracted precipitates are of the type $M_{23}$ (C, Si)$_6$. Figure 2 illustrates the temperature dependence of Fe, Cr, and Ni concentrations observed in precipitates extracted from irradiated Type 304L steel. The mole contentrations are based upon C(Ni) + C(Cr) + C(Fe) = 1. Besides the fact that Ni concentrations were found to be much higher than expected from out-of-reactor $M_{23}C_6$ precipitation data, the most notable feature found in this data is that the Ni concentration increases with decreasing irradiation temperature. This is contrary to what one would expect if Ni depletion to precipitates contributes to enhanced $\gamma \rightarrow \alpha$ transformation. Moreover, Figure 3 demonstrates that the total amount of carbide formed at a given exposure time is rather insensitive to temperature over a ~400 - 500°C temperature range. These observations demonstrate that matrix solute depletion to precipitates is an unlikely contributor to the observed $\gamma \rightarrow \alpha$ transformation in 304L. However, void nucleation in 304L was found to have reached completion by fluences of ~1 x $10^{26}$ n/m$^2$,[17] and thus these more effective sites for Ni segregation exist very early during irradiation. Therefore, Ni

segregation to voids is likely to have a stronger influence on matrix depletion than does precipitate reactions in 304L material.

In 316 stainless steel, however, void nucleation is more sluggish, and precipitation reactions are more prevalent.[6] Figures 4-7 illustrate the fluence dependence of Fe, Cr, Ni, and Mo concentrations in carbosilicides extracted from 316 creep capsule material. As in 304L, a very high Ni concentration was observed. Unlike 304L, however, the concentration was found to be higher at 550°C than at 400°C. Moreover, Table 2 illustrates that an order of magnitude more precipitation had occurred at 550°C than at 400°C for similar in-reactor times and neutron exposures, showing that matrix solute depletion is considerably greater at the higher irradiation temperature. Further, if one considers that $Ni_3Si$ also precipitates heavily at temperatures around 500°C[11] then matrix Ni depletion can be quite substantial at irradiation temperatures $\geq$ 500°C, providing conditions for pronounced $\gamma \rightarrow \alpha$ transformation. This temperature dependence of Ni depletion helps to explain the marked temperature dependence of the transformation in 316 steels. Figure 8 illustrates the temperature dependence of precipitate Ni concentration in solution-annealed 316 fueled cladding. The data indicates a peak in Ni concentration near 480°C which suggests a rapid increase in matrix Ni depletion above 400°C. The exact position of this peak, however, is questionable as the temperature of driver fuel pins decreases ~30°C during their life; the reported temperatures in Figure 8 are time-averaged temperatures.

## Conclusions

1. Both 304L and 316 stainless steels exhibit irradiation-induced $\gamma \rightarrow \alpha$ transformations with increasing propensity for transformation with temperature between 400 and 550°C.

2. Segregation of Ni solute in these steels is evidenced by unusually high Ni concentrations in irradiation-induced carbosilicide precipitates. A likely mechanism for such segregation is by a defect trapping phenomenon.

3. Type 304L material behaves differently than 316 in that Ni depletion to precipitates is more extensive at lower irradiation temperatures (~400°C). The difference can be attributed to the fact that irradiation-induced voids nucleate much more quickly in 304L and hence provide preferential sites at early times for Ni segregation. Type 316 steels therefore reflect Ni segregation to precipitates much more strongly. Ni-segregation enhancement of $\gamma \rightarrow \alpha$ transformation is therefore consistent with observed temperature dependencies of both phenomena, and the occurrence of stable $\gamma$ shells around voids in fully transformed regions of irradiated 304L material.

## REFERENCES


1. J. T. Stanley and K. R. Garr, Met Trans. A, 6A (1975) 531.

2. J. L. Baron, R. Cadalbert, and J. Deleplace, J. Nucl. Mater., 51 (1974) 266.

3. D. W. Keefer, A. G. Pard, C. G. Rhodes, and D. Kramer, J. Nucl. Mater., 39 (1971) 229.

4. D. L. Porter, J. Nucl. Mater., in press.

5. J. M. Leitnaker and J. Bentley, Met Trans. A, 8A (1977) 1605.

6. H. R. Brager and F. A. Garner, presented at the ASTM Symposium on Effects of Radiation on Structural Materials, July 10, 1978, Richland, Washington.

7. G. L. McVay, R. E. Einziger, G. L. Hofman, and L. C. Walters, J. Nucl. Mater., in press.

8. P. R. Okamoto and H. Wiedersich, J. Nucl. Mater., 53 (1974) 336.

9. D. I. Potter, L. E. Rehn, P. R. Okamoto, and H. Wiedersich, Scripta Met., 11 (1977) 1095.

10. A. Barber and A. J. Ardell, Scripta Met., 9 (1975) 1233.

11. H. R. Brager and F. A. Garner, J. Nucl. Mater., 73 (1978) 9.

12. B. Weiss and R. Stickler, Met. Trans., 3 (1972) 851.

13. H. R. Kautz and H. Gerlach, Arch. Eisenhuttenw, 2 (1968) 151.

14. M. Waldenstrom, Met. Trans. A, 8A (1977) 1963.

15. P. R. Okamoto, N. Q. Lam, H. Wiederaich, and R. A. Johnson, J. Nucl. Mater., 69-70 (1978) 821.

16. L. K. Mansur and W. G. Wolfer, J. Nucl. Mater., 69-70 (1978) 825.

17. J. E. Flinn, private communication.

Acknowledgements

The authors wish to thank J. E. Flinn for the use of unpublished data concerning some of the carbide analyses in Type 304L materials, M. K. Korenko of Hanford Engineering Development Laboratory for helpful discussions, and R. E. Einziger of Argonne National Laboratory for fuel-cladding data.

Figure Captions

Figure 1 - Dark-field electron micrograph illustrating a transformation interface between $\gamma$ and $\alpha$ phases in a partially transformed 304L steel. Note the heavy faulting in the $\gamma$ phase near the interface and the retained austenitic shells around voids as the interface passes.

Figure 2 - Temperature dependence of the chemical composition of irradiation-induced carbosilicides - $M_{23}(C, Si)_6$ - in 304L material.

Figure 3 - Time dependence of the amount of irradiation-induced precipitation in 304L steel. Note that the amount of precipitation is quite insensitive to irradiation temperature.

Figure 4 - Fluence dependence of Ni and Mo concentrations in extracted precipitates of 550°C - irradiated 316 stainless steel creep capsule material.

Figure 5 - Fluence dependence of Fe and Cr concentrations in extracted precipitates of 550°C - irradiated 316 stainless steel creep capsule material.

Figure 6 - Fluence dependence of Ni and Mo concentrations in extracted precipitates of 400°C _ irradiated 316 stainless steel creep capsule material.

Figure 7 - Fluence dependence of Fe and Cr concentrations in extracted precipitates of 400°C - irradiated 316 stainless steel creep capsule material.

Figure 8 - Temperature dependence of Ni concentrations in irradiation-induced precipitates extracted from fuel-cladding material (solution-annealed 316). Also shown are averaged compositions for precipitates extracted from 316 creep capsule material (number of specimens averaged is in parenthesis). Scatter in the data at high temperatures resulted from fuel-cladding chemical interaction.

TABLE 1 - CHEMICAL COMPOSITIONS OF STAINLESS STEELS INVESTIGATED

| | C | Mn | P | S | Si | Ni | Cr | Ti | Cu | Mo | Co |
|---|---|---|---|---|---|---|---|---|---|---|---|
| 304L: | 0.03 | 1.37 | 0.01 | 0.007 | 0.62 | 9.26 | 18.3 | 0.02 | 0.074 | 0.02 | 0.05 |
| 316 (N-LOT): | 0.07 | 1.42 | 0.02 | 0.01 | 0.47 | 13.57 | 16.36 | NA | NA | 2.88 | NA |
| 316 (FUELED): | 0.055 | 1.67 | 0.004 | 0.006 | 0.54 | 13.64 | 17.45 | NA | NA | 2.30 | NA |

TABLE 2

CARBIDE PRECIPITATION IN TYPE 316 STAINLESS STEEL FROM NONFUELED EXPERIMENTS[a]

| Sample Description | Temp. (°C) | Neutron Fluence ($10^{26}$ n/m$^2$) | Hoop Stress (Mpa) | N[b] | Time at Temp. (in Reactor) hrs. |
|---|---|---|---|---|---|
| 20% Cold-worked | | | | | |
| Unirradiated | --- | 0 | 0 | $1.4 \times 10^{-4}$ | 0 |
| Irradiated | 400 | 4.2 | 0 | $5.0 \times 10^{-4}$ | 22,802 |
| Irradiated | 400 | 4.4 | 276 | $5.1 \times 10^{-4}$ | 22,802 |
| Irradiated | 550 | 3.8 | 103 | $8.3 \times 10^{-3}$ | 10,767 |
| Soln. Ann. | | | | | |
| Unirradiated | --- | 0 | 0 | ( $1 \times 10^{-5}$) | 0 |
| Irradiated | 400 | 4.6 | 276 | $8.2 \times 10^{-4}$ | 26,448 |

[a]The material analyzed for these results was obtained from creep experiments utilizing He-filled Type 316 stainless steel capsules in a variety of metallurgical conditions.

[b]Ratio of the weight of metal ions (Fe, Cr, Ni, and Mo) found in the carbide precipitates to the sample weight tested. Each value of N is an average of the results from two or more samples.

Fig. 1


Fig 1

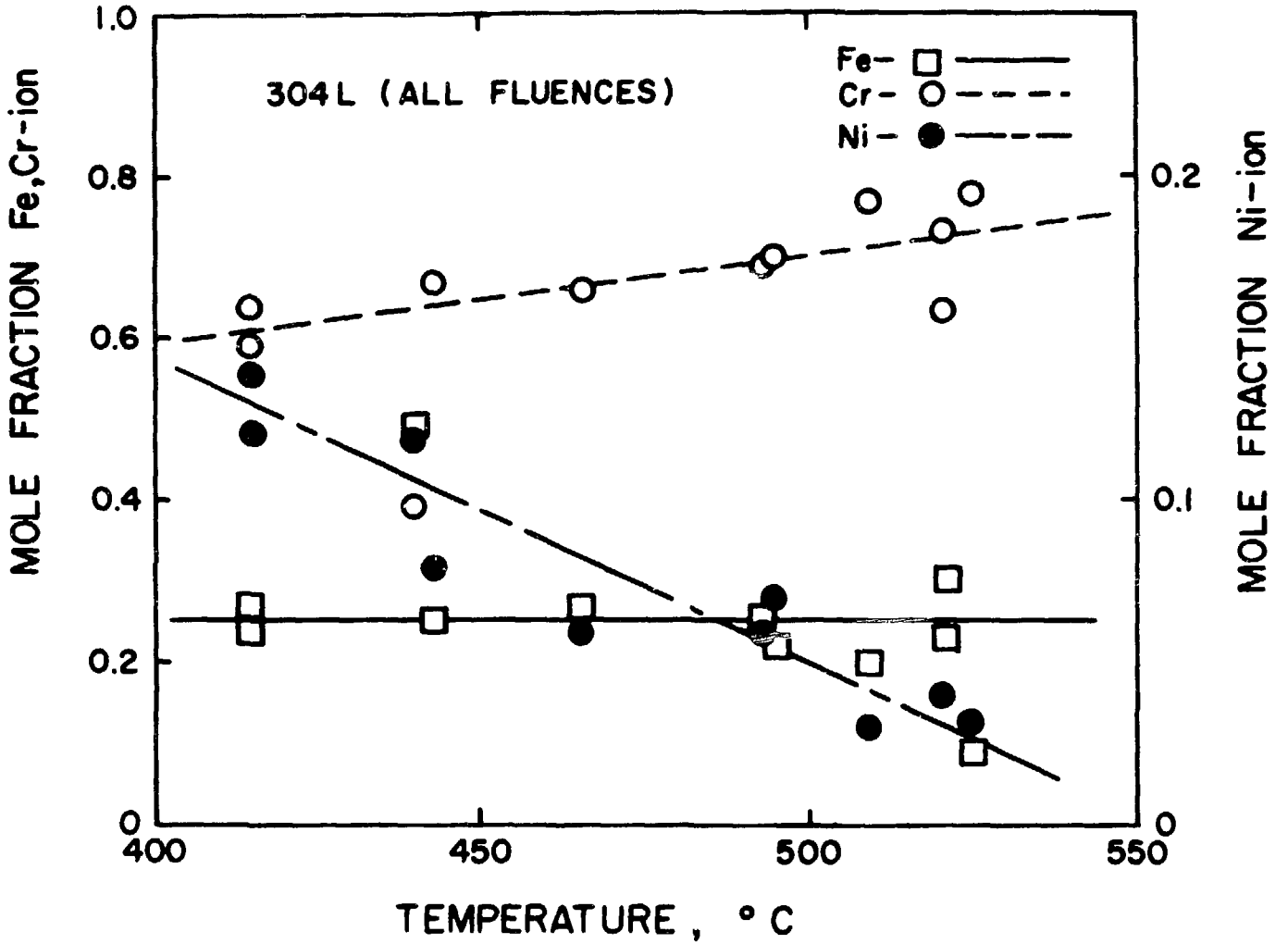
304 L (ALL FLUENCES)
Fe-
Cr-
Ni-
MOLE FRACTION Fe,Cr-ion
MOLE FRACTION Ni-ion
TEMPERATURE , °C
1.0
0.8
0.6
0.4
0.2
0
0.2
0.1
0
400
450
500
550

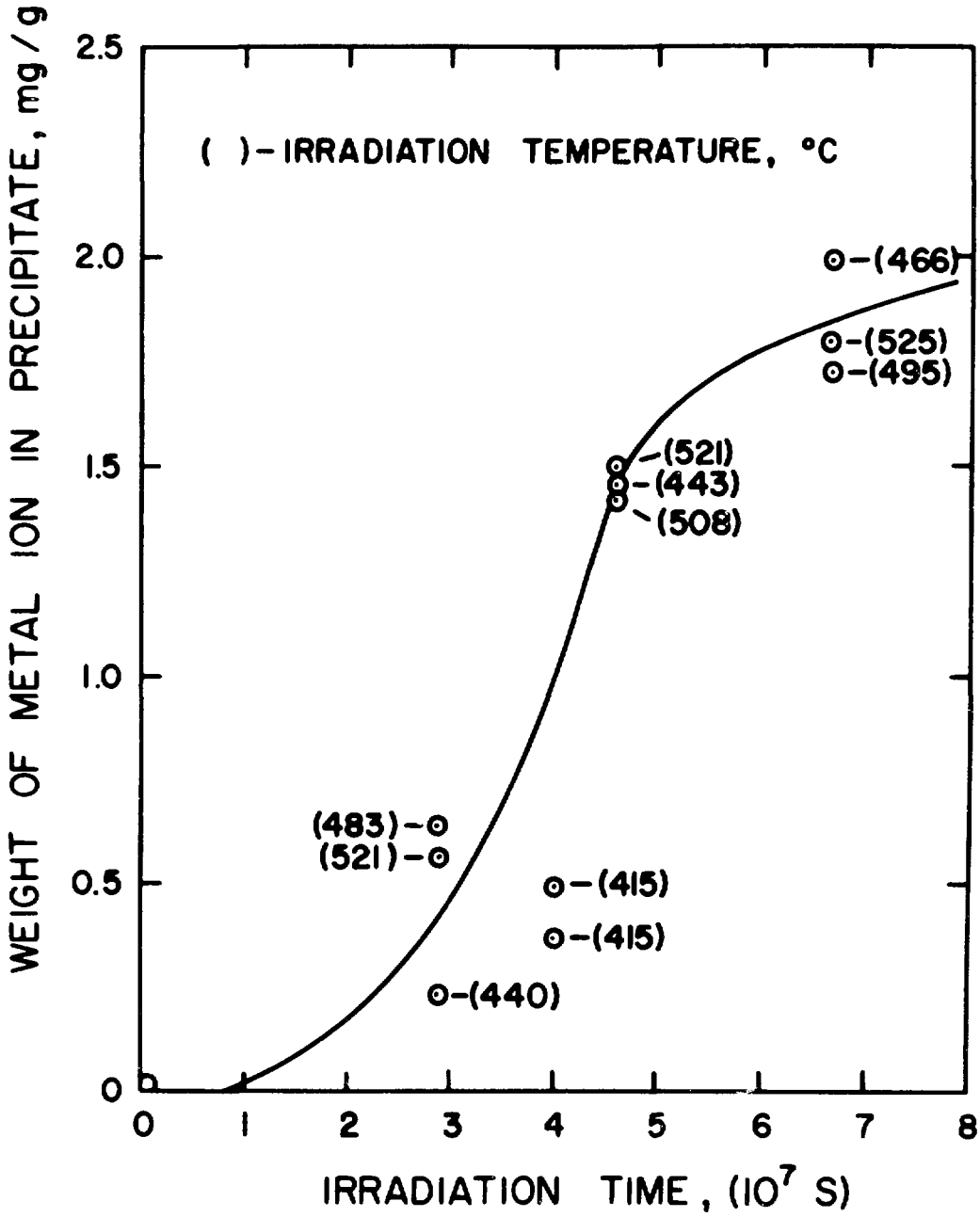
( )-IRRADIATION TEMPERATURE, °C
⊙-(466)
⊙-(525)
⊙-(495)
⊙-(521)
⊙-(443)
⊙-(508)
(483)-⊙
(521)-⊙
⊙-(415)
⊙-(415)
⊙-(440)
WEIGHT OF METAL ION IN PRECIPITATE, mg/g
IRRADIATION TIME, ($10^7$ S)
0
0.5
1.0
1.5
2.0
2.5
0
1
2
3
4
5
6
7
8

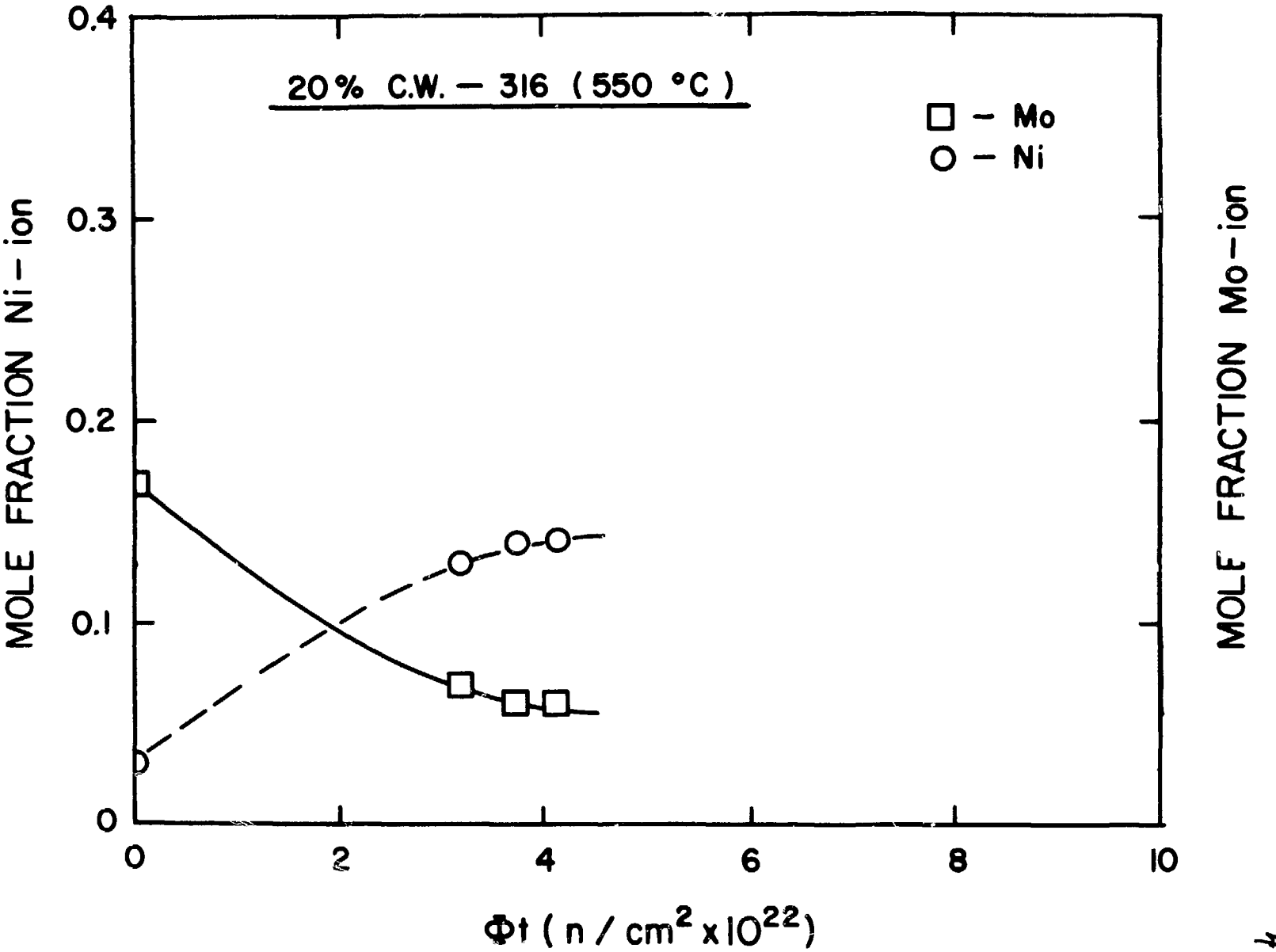
20% C.W. — 316 (550 °C)
□ – Mo
○ – Ni
MOLE FRACTION Ni – ion
MOLE FRACTION Mo – ion
0.4
0.3
0.2
0.1
0
0
2
4
6
8
10
Φt ( n / cm² x 10²²)

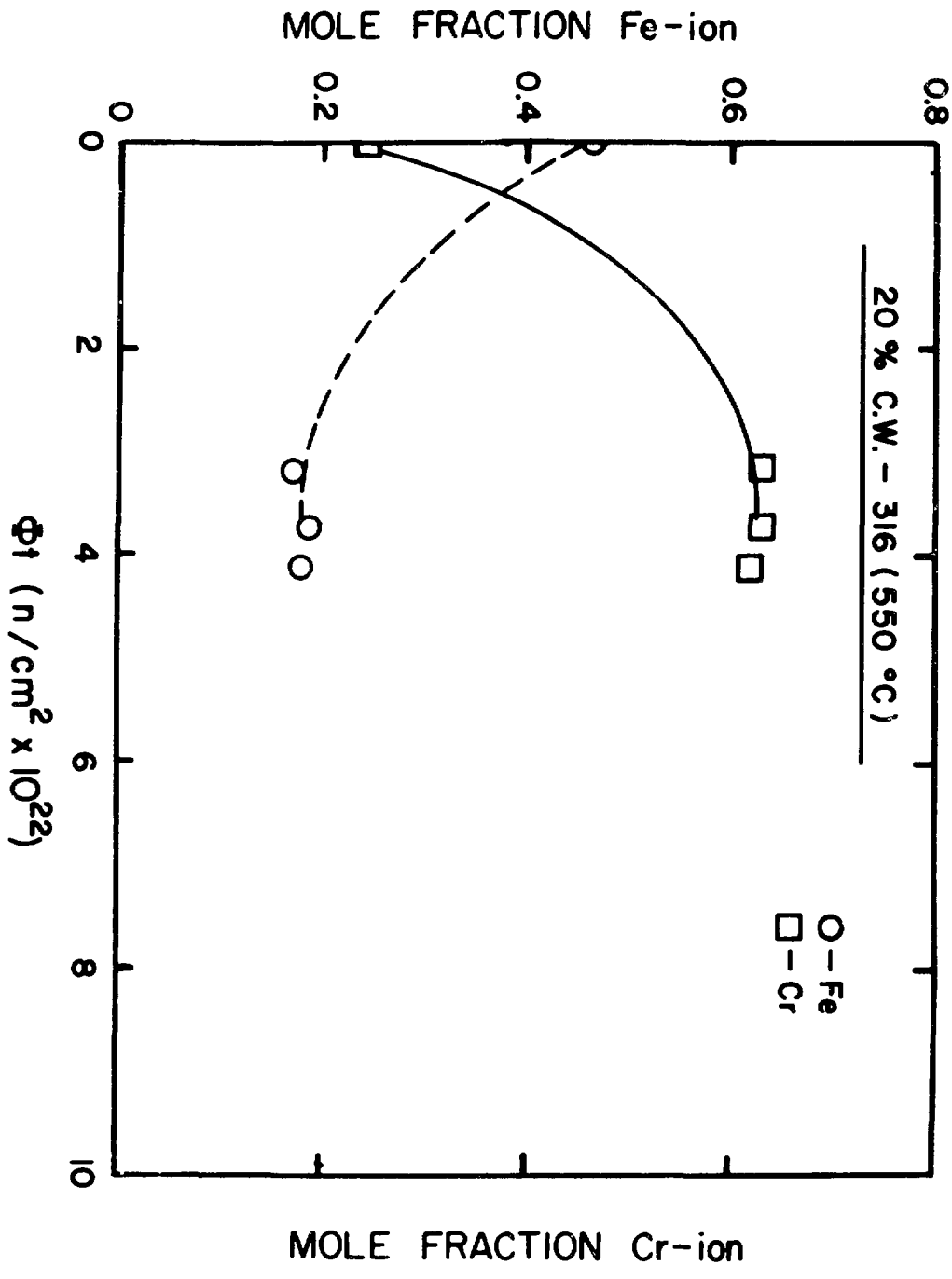
MOLE FRACTION Fe-ion
0
0.2
0.4
0.6
0.8
0
2
4
6
8
10
Φt (n/cm² x 10²²)
20 % C.W. - 316 (550 °C)
O - Fe
□ - Cr
MOLE FRACTION Cr-ion

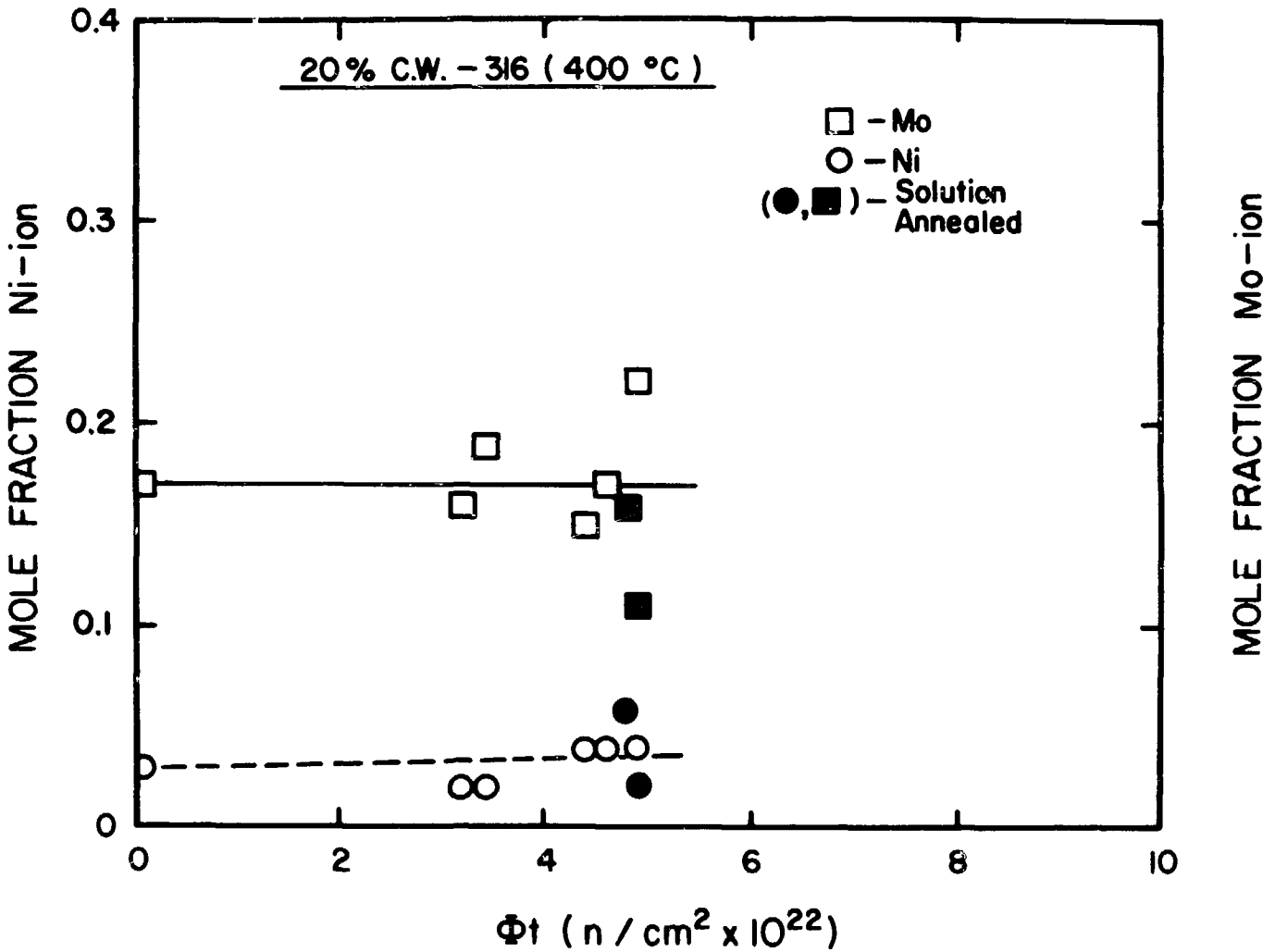
20% C.W. – 316 (400 °C)
□ – Mo
○ – Ni
(●,■) – Solution Annealed
MOLE FRACTION Ni-ion
MOLE FRACTION Mo-ion
0.4
0.3
0.2
0.1
0
0
2
4
6
8
10
Φt (n / cm² x 10²²)

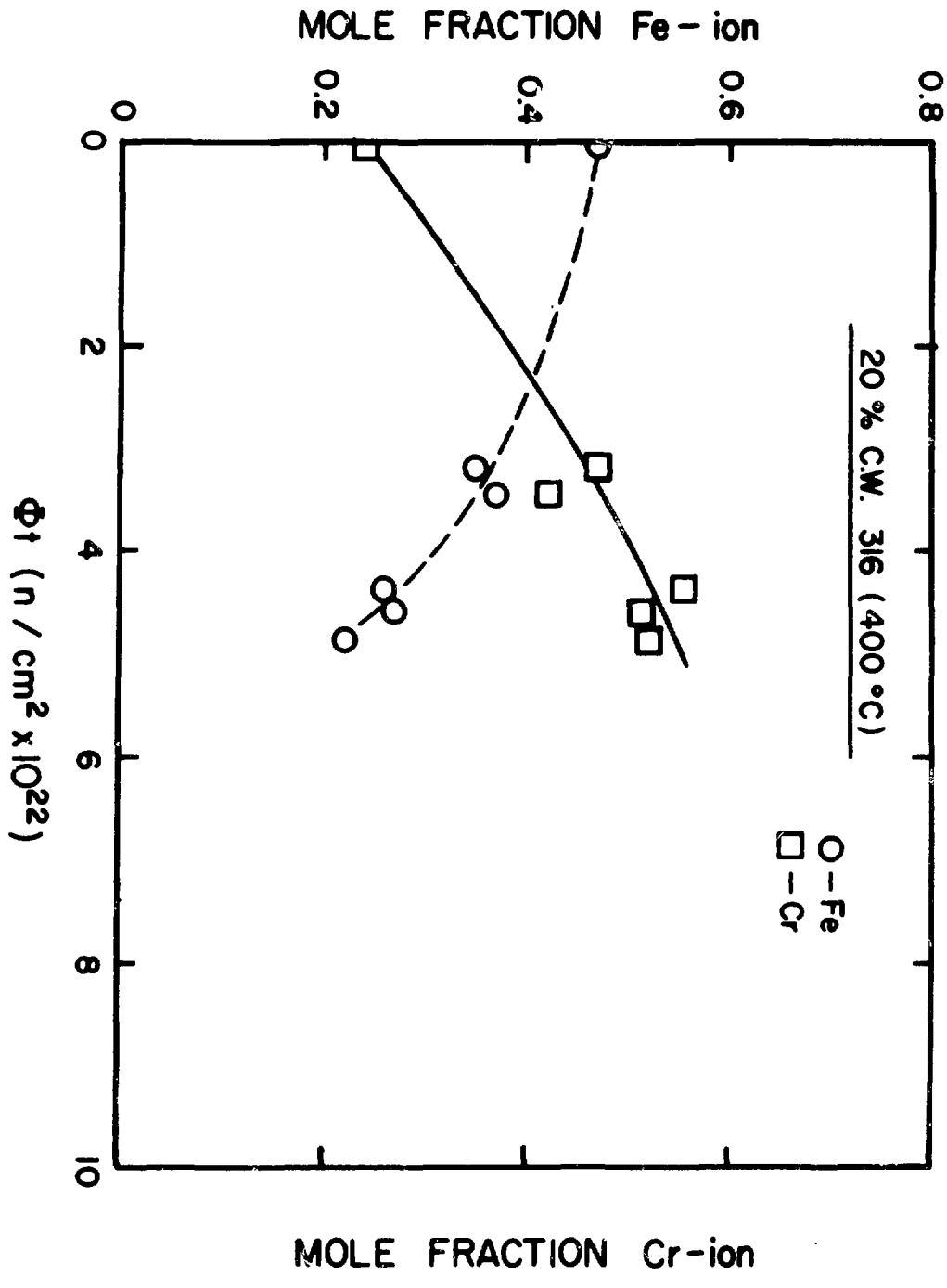
MOLE FRACTION Fe - ion
0
0.2
0.4
0.6
0.8
0
2
4
6
8
10
Φt (n / cm² x 10²²)
20 % C.W. 316 (400 °C)
O - Fe
□ - Cr
MOLE FRACTION Cr-ion

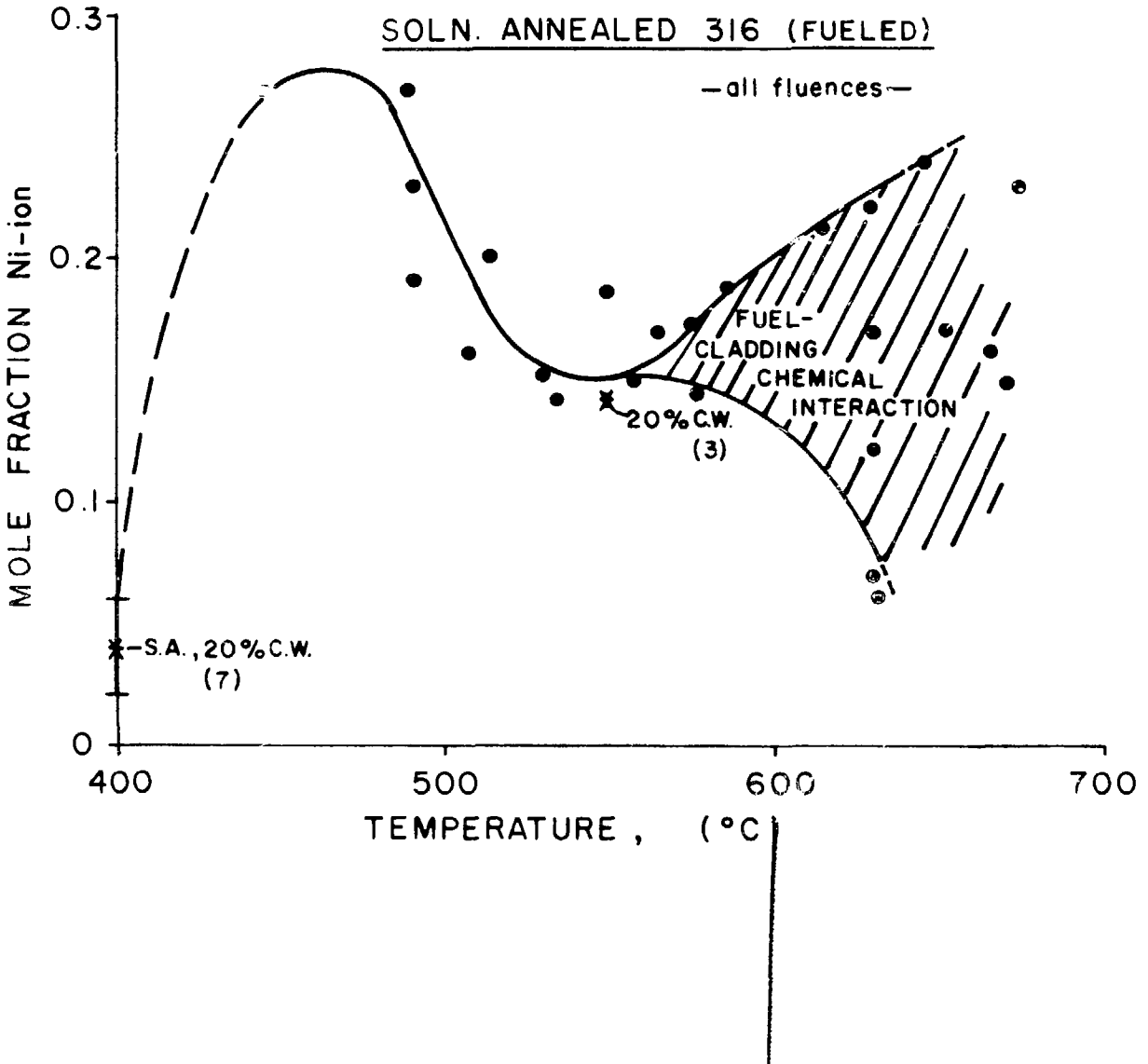
SOLN. ANNEALED 316 (FUELED)
—all fluences—
MOLE FRACTION Ni-ion
0.3
0.2
0.1
0
400
500
600
700
TEMPERATURE, (°C)
FUEL-CLADDING CHEMICAL INTERACTION
20% C.W. (3)
S.A., 20% C.W. (7)